MOLECULAR ONCOLOGY 7 (2013) 428–439

available at www.sciencedirect.com

SciVerse ScienceDirect

www.elsevier.com/locate/molonc

Plumbagin, a medicinal plant (*Plumbago zeylanica*)-derived 1,4-naphthoquinone, inhibits growth and metastasis of human prostate cancer PC-3M-luciferase cells in an orthotopic xenograft mouse model

Bilal Bin Hafeez[a,*], *Weixiong Zhong*[b], *Joseph W. Fischer*[a], *Ala Mustafa*[a], *Xudong Shi*[c], *Louise Meske*[a], *Hao Hong*[d], *Weibo Cai*[d], *Thomas Havighurst*[e], *KyungMann Kim*[e], *Ajit K. Verma*[a]

[a]*Department of Human Oncology, Paul Carbone Comprehensive Cancer Center, School of Medicine and Public Health, University of Wisconsin, Madison, WI 53792, USA*
[b]*Department of Pathology, Paul Carbone Comprehensive Cancer Center, School of Medicine and Public Health, University of Wisconsin, Madison, WI 53792, USA*
[c]*Department of Surgery, Paul Carbone Comprehensive Cancer Center, School of Medicine and Public Health, University of Wisconsin, Madison, WI 53792, USA*
[d]*Department of Radiology, Wisconsin Institute for Medical Research, Paul Carbone Comprehensive Cancer Center, School of Medicine and Public Health, University of Wisconsin, Madison, WI 53792, USA*
[e]*Department of Biostatistics & Medical Informatics, Paul Carbone Comprehensive Cancer Center, School of Medicine and Public Health, University of Wisconsin, Madison, WI 53792, USA*

ARTICLE INFO

Article history:
Received 3 December 2012
Accepted 4 December 2012
Available online 14 December 2012

Keywords:
Plumbagin
Prostate cancer
Orthotopic xenograft model

ABSTRACT

We present here first time that Plumbagin (PL), a medicinal plant-derived 1,4-naphthoquinone, inhibits the growth and metastasis of human prostate cancer (PCa) cells in an orthotopic xenograft mouse model. In this study, human PCa PC-3M-luciferase cells (2×10^6) were injected into the prostate of athymic nude mice. Three days post cell implantation, mice were treated with PL (2 mg/kg body wt. i.p. five days in a week) for 8 weeks. Growth and metastasis of PC-3M-luciferase cells was examined weekly by bioluminescence imaging of live mice. PL-treatment significantly ($p = 0.0008$) inhibited the growth of orthotopic xenograft tumors. Results demonstrated a significant inhibition of metastasis into liver ($p = 0.037$), but inhibition of metastasis into the lungs ($p = 0.60$) and lymph nodes ($p = 0.27$) was not observed to be significant. These results were further confirmed by histopathology of these organs. Results of histopathology demonstrated a significant inhibition of metastasis into lymph nodes ($p = 0.034$) and lungs ($p = 0.028$), and a trend to significance in liver ($p = 0.075$). None of the mice in the PL-treatment group showed PCa metastasis into the liver, but these mice had small metastasis foci into the lymph nodes and lungs. However, control mice had large metastatic foci into the lymph nodes, lungs, and liver. PL-caused inhibition of the growth and metastasis of PC-3M cells accompanies inhibition of the expression of: 1) PKCε, pStat3Tyr705, and pStat3Ser727, 2) Stat3

Abbreviations: PL, plumbagin; PCa, prostate cancer; PKCε, protein kinase C epsilon; Stat3, signal transducers and activators of transcription 3.

* *Corresponding author*. Tel.: +1 608 262 1744; fax: +1 608 262 6654.
E-mail addresses: indianbilal@yahoo.com, hafeez@humonc.wisc.edu (B.B. Hafeez).

1574-7891/$ – see front matter Published by Elsevier B.V. on behalf of Federation of European Biochemical Societies.
http://dx.doi.org/10.1016/j.molonc.2012.12.001

downstream target genes (survivin and Bcl_{xL}), 3) proliferative markers Ki-67 and PCNA, 4) metastatic marker MMP9, MMP2, and uPA, and 5) angiogenesis markers CD31 and VEGF. Taken together, these results suggest that PL inhibits tumor growth and metastasis of human PCa PC3-M-luciferase cells, which could be used as a therapeutic agent for the prevention and treatment of human PCa.

Published by Elsevier B.V. on behalf of Federation of European Biochemical Societies.

1. Introduction

Prostate cancer (PCa) continues to remain the most common cancer and the second leading cause of cancer-related deaths in American men. The American Cancer Society has predicted that a total of 241,740 new cases of PCa will be diagnosed and 28,170 deaths will occur from it in the United States alone in the year of 2012 (Siegel et al., 2012). Although PCa is frequently curable in its early stage by surgical or radiation therapy, many patients present locally advanced or metastatic disease for which there are currently no curative treatment option (Albertsen, 2008; So et al., 2005). Therefore, there is an urgent need for agents, which are effective and selective, in the prevention and/or treatment of PCa metastasis.

PL is a quinoid (5-hydroxy-2-methyl-1,4-napthoquinone) constituent isolated from the roots of the medicinal plant *Plumbago zeylanica* L. (also known as Chitrak) (Sandur et al., 2006). PL has also been found in *Juglans regia* (English Walnut), *Juglans cinerea* (butternut and white walnut) and *Juglans nigra* (blacknut) (Sandur et al., 2006). The root of *P. zeylanica* has been used in traditional Indian and Chinese systems of medicine for more than 2500 years for the treatment of various types of ailments (Sandur et al., 2006). PL has been shown for its potential health benefits including neuroprotective (Son et al., 2010) and anti-cancer property against various types of cancers (Padhye et al., 2012 and references therein). PL, fed in the diet (200 ppm), inhibits azoxymethane-induced intestinal tumors in rats (Courboulin et al., 2012). PL inhibits ectopic growth of human breast cancer (Sugie et al., 1998), non-small cell lung cancer (Hsu et al., 2006), melanoma (Wang et al., 2008), and ovarian (Sinha et al., 2012) cells in athymic nude mice. We have shown that PL inhibits ultraviolet radiation-induced development of squamous cell carcinomas (Ravindra et al., 2009). We including others have also reported its apoptosis inducing and growth inhibitory effects against pancreatic cancer (Hafeez et al., 2012a; Lai et al., 2012) and PCa (Aziz et al., 2007a; Gomathinayagam et al., 2008; Powolny and Singh, 2008) cells. Recently, we have reported that PL inhibits prostate tumor growth in transgenic adenocarcinoma of mouse prostate (TRAMP) mice (Hafeez et al., 2012b). However, no study has demonstrated anti-metastasis potential of PL against human PCa. We present in this communication, for the first time, that PL administration inhibits metastatic growth of human PCa PC-3M-luciferase cells in an orthotopic xenograft mouse model. PL-caused inhibition of the growth and metastasis of PC-3M-luciferase cells accompanies inhibition of the expression of PKCε, pStat3-Tyr705, and pStat3Ser727, Stat3 downstream target genes (survivin and Bcl_{xL}), proliferative markers (Ki-67 and PCNA), metastatic markers (MMP2, MMP9 and uPA), angiogenesis markers (CD31 and VEGF) and induction of iNOS expression.

2. Materials and methods

2.1. Antibodies

Monoclonal or polyclonal antibodies specific for actin, CD31, E-Cadherin, iNOS, Ki-67, MMP9, MMP2, PKCε, PCNA, survivin, total Stat3, uPA, and VEGF were purchased from Santa Cruz Biotechnology, (Santa Cruz, CA). Monoclonal antibodies specific for pStat3Tyr705, and pStat3Ser727 were obtained from BD Biosciences (San Jose, CA). PL (Practical grade, purity: 99.80% HPLC, molecular weight: 188.18) was purchased from Sigma–Aldrich (St. Louis, MO).

2.2. Orthotopic xenograft

PC-3M-luciferase cells were obtained from Caliper Life Sciences (Hopkinton, MA). Six weeks old male athymic nude mice, purchased from Harlan Laboratory (Madison, WI), were housed under pathogen-free environment with a 12 h light/12 h dark schedule and fed with an autoclaved diet and water *ad libitum*. To establish orthotopic xenografts in mice, PC-3M-luciferase cells (2.0×10^6) were suspended in 20 μl of HBSS media and directly implanted into the anterior lobe of the prostate. Three days later, 16 mice were randomly divided into two groups. One group of mice ($n = 8$) was treated with an i.p. injection of PL (2 mg/kg body weight in 0.1 ml PBS, once a day and 5 days per week for 8 weeks). Control mice ($n = 8$) were treated the same with vehicle (0.1 ml PBS). The mice were maintained at the AAALAC-accredited Animal Resources Facility of the University of Wisconsin. All of the protocols were approved by the University's Research Animal Resources Committee in accordance with the NIH Guideline for the Care and Use of Laboratory Mice.

2.3. Bioluminescence imaging

Mice of both the groups were imaged weekly using an IVIS Spectrum scanner (formerly Caliper Life Sciences now PerkinElmer, Waltham, MA). In brief, 200 μl of substrate D-luciferin (3.0 mg) in PBS was injected i.p. in each mouse at 10 min prior to imaging. Images were quantified and normalized by using vendor software (Living Image® 4.0). Regions-of-interest (ROI) of the same size and shape were used for all mice throughout the study. The bioluminescence images were quantified by measuring the total photons over the prostate region and the average photon flux within the ROI were presented as photons/second/cm^2/sr (sr denotes steradian). To determine the metastasis into the distant organs, entire excised organs (liver, lymph nodes, lungs, and bone) were kept in 6-well plates, imaged and quantified as described above.

2.4. Histopathological examination

Prostate tumors, lungs, liver, and lymph nodes from both of the groups were excised and processed for histology as described previously (Aziz et al., 2007a). Dr. Weixiong Zhong, a certified pathologist in the Department of Pathology, University of Wisconsin School of Medicine and Public Health, examined all of the tissue slides.

2.5. Western blot analysis

Part of the excised prostate tumor tissues from each group mice were used to prepared whole tissue lysates. In brief, prostate tissues were homogenized in lysis buffer [50 mmol/LHEPES, 150 mmol/L NaCl, 10% glycerol, 1% Triton X-100, 1.5 mmol/L$MgCl_2$, 10 μg/mL aprotinin, 10 μg/mL leupeptin, 1 mmol/L phenylmethylsulfonyl fluoride (PMSF), 200 μmol/L Na_3VO_4, 200 μmol/L NaF, and 1 mmol/L EGTA (final pH 7.5)]. The homogenates were centrifuged at 14,000 × *g* for 30 min at 4 °C. Supernatants were collected and stored at −80 °C until further use. Protein concentration was estimated by using Bio-Rad protein assay kit as per the manufacturer's protocol. Fifty micrograms of cell lysate were fractionated on 10–15% Criterion precast SDS-polyacrylamide gels (Bio-Rad Laboratories, Hercules CA). The fractionated proteins were transferred to 0.45 μm Hybond-P polyvinylidene difluoride (PVDF) transfer membrane (Amersham Life Sciences, Piscataway NJ). The membrane was then incubated with the specific antibody followed by the appropriate horseradish peroxidase-conjugated secondary antibody (Thermo Scientific, Pittsburgh, PA), and the detection signal was developed with Amersham's enhanced chemiluminescence reagent and using FOTO/Analyst Luminary Work Station (Fotodyne Inc., Hartland, WI). The Western blots were quantified by densitometric analysis using Total lab Nonlinear Dynamic Image analysis software (Nonlinear USA, Inc., Durham, NC).

2.6. Immunohistochemistry

To determine the expression of CD31, E-cadherin, Ki-67, and PCNA proteins in excised orthotopic xenograft tumors of control and PL-treated mice, we performed immunohistochemistry in paraffin embedded sections (4 μm thickness). In brief, sections were deparaffinized by placing the slides at 60 °C for 2 h followed by 3 changes of Xylene for 10 min each. Slides were placed in 0.3% methanol/Hydrogen peroxide for 20 min for quenching endogenous peroxidase. Slides were rehydrated in one change of absolute, 95%, 75%, and 50% ethanol and distilled water. Antigen retrieval was performed by incubating samples at 116 °C for 15 s in the declocking chamber by using a Tris–urea solution (pH 9.5). After antigen retrieval, tissues slides were incubated with 2.5% normal horse serum (R.T.U. Vectastain Universal Elite ABC Kit, Vector Laboratories, Burlingame, CA) for 20 min to block non-specific binding of the antibodies. Subsequently, the slides were incubated over night with a mixture of E-cadherin (1:50), Ki-67 (1:50) and PCNA (1:50) dilution in normal antibody diluents (Scy Tek # ABB-125, Logan, UT) in a humidified chamber. Specificity of immunostaining of these proteins was confirmed by using IgG antibody (served as a negative control). The mixture of antibodies was decanted and the slides were washed thrice in TBS (pH7.4). The slides were incubated with appropriate secondary antibodies for 30 min at room temperature. Slides were rinsed with TBS for 5 min and ABC reagent (Vector kit) was applied for 30 min. Immunoreactive complexes were detected using DAB substrate (Thermo Scientific, Pittsburgh, PA), and counter stained by using hematoxylin (Fischer Scientific, Pittsburgh, PA) for nuclear staining. Finally, slides were mounted with a cover slip by using mounting medium. All sections were visualized under a Zeiss-Axiophot DM HT microscope and images captured with an attached camera.

2.7. Immunofluorescence

Paraffin-fixed orthotopic xenograft tumors tissue sections (4-μm thick) from control and PL-treated mice were used to determine the expression of VEGF. After antigen retrieval by incubating samples at 95 °C in Tris–urea solution (pH 9.5) for 30 min, the tissue slides were incubated with normal horse serum (1:10 dilution) for 30 min to block nonspecific binding of the antibodies. Subsequently, the slides were incubated overnight with VEGF (1:50 dilution) primary antibody in a humidified chamber. The mixture of antibodies was decanted and the slides were washed thrice in 1× TBS (pH 7.4). The slides were incubated with FITC-labeled secondary antibody for 1 h at room temperature in the dark. The solution of secondary antibody was decanted and the slides were washed thrice with TBS for 5 min intervals each in the dark. Finally, the specimens were mounted with coverslips using a drop of mounting medium containing DAPI (Vector Lab, Inc., Burlingame, CA). Similar procedure was followed to determine the effect of PL on CD31 expression. All sections were examined with an Olympus Microscope attached with fluorescence detector.

2.8. Statistical analysis

Bioluminescence values for the primary tumor were recorded weekly for 8 weeks beginning three days after the start of treatment. Bioluminescence imaging was also performed on excised liver, lungs and lymph nodes at the end of the study. The normality of the bioluminescence imaging data was assessed; log-transformed values were found to conform to normality assumptions better than raw values and subsequent analyses used log-transformed measures. Differences between treatment arms for ordered categorical data such as histopathological analysis were tested using the Wilcoxon rank-sum test. Differences between the two treatment arms for continuous data were tested using the Wilcoxon rank-sum test or Student's *t*-test on the transformed data as appropriate. Mixed-effects models for repeated measures of the log-transformed bioluminescence data were built using the SAS procedure GLIMMIX, using an autoregressive covariance structure, which was chosen for these models using Akaike's Information Criteria. Computations were performed with SAS (1A) and R (2A) software; figures were created with R software. (Version 9.2 of the SAS System for [Unix]. Copyright© 2002–2008 SAS Institute Inc. SAS and all other SAS Institute Inc. product or service names are registered trademarks or trademarks of SAS Institute Inc., Cary, NC, USA)(Core Development Team, 2011).

3. Results

3.1. PL-treatment inhibits growth and metastasis of PC-3M-luciferase cells orthotopic xenograft tumors in athymic nude mice

To precisely monitor the effects of PL on the growth and metastasis of PC-3M-luciferase cells in live mice, cells were implanted into the mouse prostate. In this experiment, sixteen mice were used. Three days after PC-3M cell implantation, mice were randomly divided into two groups. One group of mice received PL-treatment (2 mg/kg body weight i.p. once a day and five days a week) and the other group of mice received only the vehicle (0.1 ml of PBS). Treatment was given upto 8 weeks and was stopped 24 h before sacrificing these mice. No apparent toxicity was observed in any of the PL-treated mouse as we observed time dependent increase in the body weight (supplementary Figure 1). Orthotopic growth of prostate tumors of both the groups was monitored weekly by bioluminescence imaging of live mice. The bioluminescence imaging results indicated a significant ($p = 0.0008$) decrease in the prostate tumor volume of PL-treated mice compared to vehicle treated mice (Figure 1A–B). The differences in the prostate tumor volume was significant shortly after the beginning of treatment; significant or near significant differences were observed at weeks 1 ($p = 0.0031$), 2 ($p = 0.0004$), 7 ($p = 0.058$), and 8 ($p = 0.027$) (Figure 1B). At 8 week, we euthanized all of the mice; their orthotopic xenograft tumors were excised, imaged, and weighed. PL-treatment showed a significant ($p = 0.006$) decrease in the bioluminescence signal intensity (Figure 1C) and tumor weight ($p = 0.006$) (Figure 1D) compared to control mice. These results were in concordance with the findings from bioluminescence imaging of live mice (Figure 1A–B).

To determine the effects of PL-treatment on PCa metastasis, we excised distant organs (liver, lungs, lymph nodes, and bones) of both the groups' mice and imaged. All of the mice from the control group showed high incidence of metastasis into distant organs, which was reduced in PL-treated mice. As shown in Figure 2, increased bioluminescence signal intensity was observed in the liver (Figure 2Ai, B), lungs (Figure 2Aiii, B), and lymph nodes (Figure 2Av, C) of control

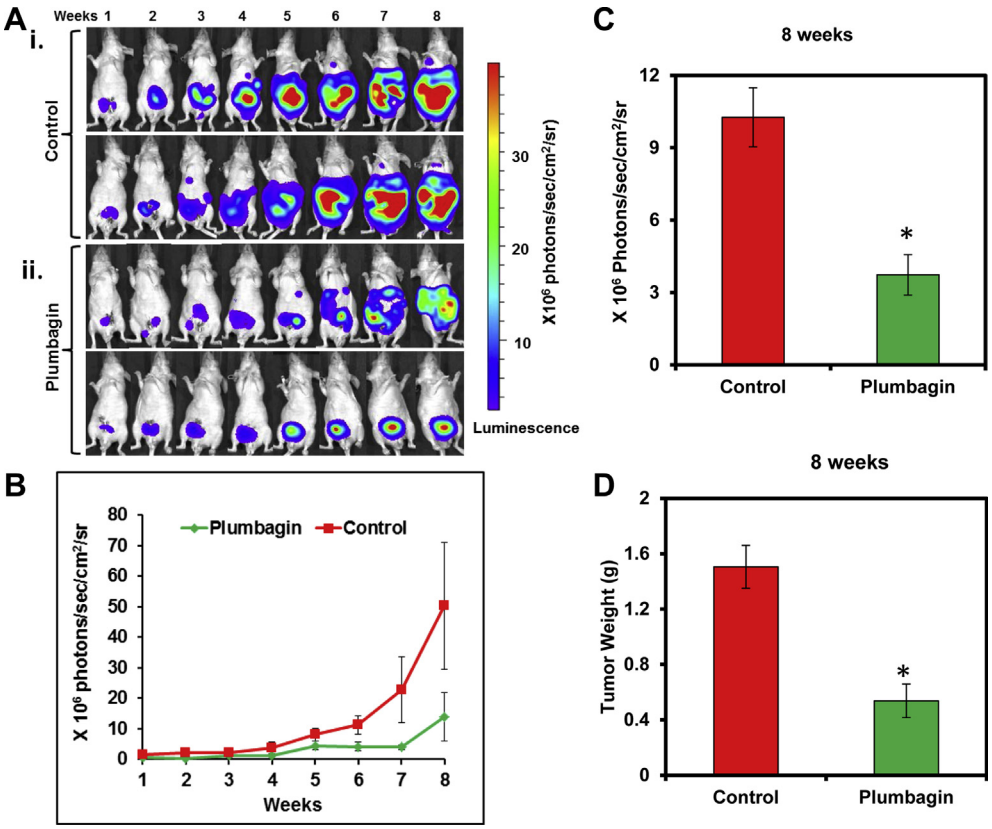

Figure 1 – Effects of PL-treatment on PC-3M-luciferase cell-derived orthotopic xenograft tumors in athymic nude mice. A and B: Luciferase labeled PC-3M cells (2×10^6) were orthotopically implanted in athymic nude mice. PL (2 mg/kg body weight) and vehicle treatment was started 3 days post-implantation. There were eight mice per group. Bioluminescence imaging of live mice was performed at the indicated weeks as described in the Methods section. Shown are two representative images of the anesthetized mice from control (Ai) and PL-treated (Aii) groups. All images were displayed at the same scale. B. The bioluminescence values (photons/sec/cm^2/sr) of the prostate region were quantified for each group of mice and mean values ± SE are plotted over time. C. Mice from both groups were sacrificed at 8 week, their prostates were excised and imaged immediately. Bar graph represents the bioluminescence values (photons/sec/cm^2/sr) of the excised prostates from control and PL-treated mice. D. Bar graph represents prostate tumor weights of control and PL-treated mice. Each value in the graph is the mean ± SE from eight mice. $^*p < 0.05$ was considered as significant.

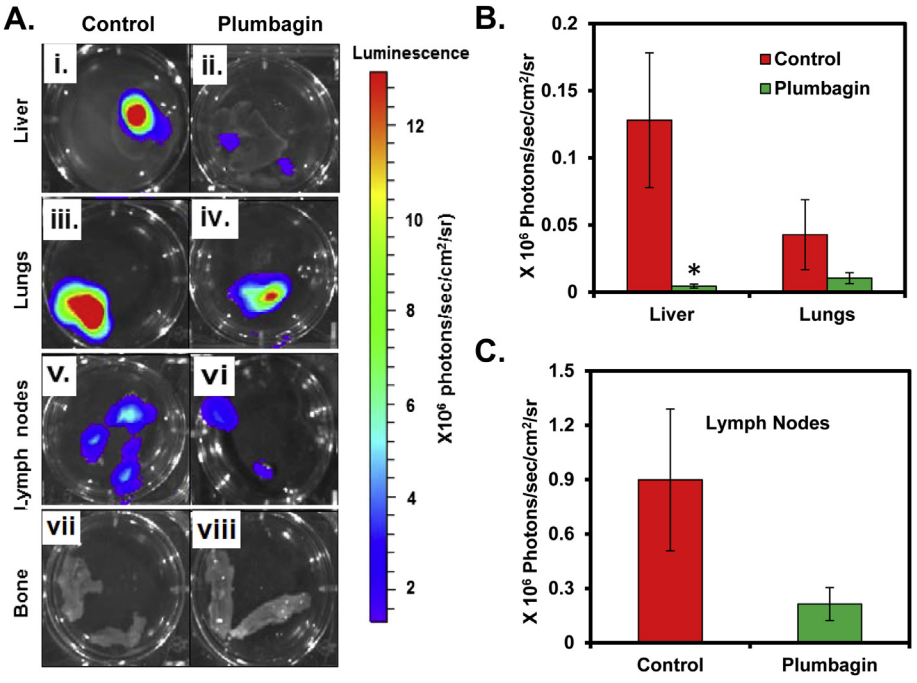

Figure 2 – Effect of PL-treatment on metastatic growth of PC-3M-luciferase cell-derived tumors in athymic nude mice. At 8 week, livers, lungs, lymph nodes and bone from both vehicle and PL-treated mice were excised and imaged. A: Representative bioluminescence images of excised livers (Ai–ii), lungs (Aiii–iv), lymph nodes (Av–vi), and bone (Avii–viii) from vehicle ($n = 8$) and PL-treated ($n = 8$) mice. The bioluminescence images of the excised liver, lungs (B) and lymph nodes (C) and bone were quantified for each group of mice. Each value in the graph (B and C) is the mean ± SE from eight mice.

mice, which was significantly decreased in the excised liver ($p = 0.037$) (Figure 2Aii, B), but not significantly decreased in lungs ($p = 0.60$) (Figure 2Aiv, B) and lymph nodes ($p = 0.27$) (Figure 2Avi, C) of PL-treated mice. None of the mice from the control or PL-treatment group showed metastasis into the bones (Figure 2Avii–viii).

We further performed histopathological analysis of excised orthotopic tumors, liver, lungs, and lymph nodes of both groups' mice. Histopathological examination of excised orthotopic tumors from both groups confirmed their growth in the mouse prostate (Figure 3Ai, Bi). Histopathological findings of lungs, liver and lymph nodes of both groups of mice are summarized in Figure 4. We observed a significant decrease of PCa metastasis into the lungs ($p = 0.028$) (Figure 4A), lymph nodes ($p = 0.034$) (Figure 4B), and a trend toward significance for liver ($p = 0.075$) (Figure 4C) in PL-treated mice compared to control. A total of 87.5% of the control mice showed lungs metastasis (Figure 3Aii and 4A). Fifty percent of the control mice had multiple metastatic foci into the lungs, while 37% mice showed scattered single cells or small groups of cells metastasized into the lungs (Figure 3Aii and 4A). None of the PL-treated mice showed multiple metastatic foci into the lungs (Figure 3Bii) and only 50% had scattered single metastatic cells or small groups of metastatic cells (Figure 4A). PL-treatment also inhibited PCa metastasis into lymph nodes compared to control group mice. All of the control mice showed lymph node metastasis (Figure 3iii and 4B). Among them 60% showed multiple metastatic foci and 40% had scattered small groups of metastases (Figure 4B). However, 75% of PL-treated mice showed lymph nodes metastasis (Figure 4B) but these metastatic cells were observed as scattered cells or small cell groups (Figure 3Biii). None of the mice in PL-treated groups showed metastasis into the liver (Figure 3Biv), while 40% of the control mice showed liver metastasis (Figure 3Aiv).

3.2. *PL-treatment inhibits PKCε and phosphorylated Stat3 expression in orthotopic prostate tumors*

We have previously reported that expression level of PKCε and Stat3 correlates with human PCa aggressiveness (Aziz et al., 2007a). Results from the experiments, involving reciprocal immunoprecipitation and pull-down assays using recombinant PKCε and Stat3, indicate that PKCε mediates Stat3Ser727 phosphorylation essential for both Stat3 DNA-binding and transcriptional activity (Aziz et al., 2007a). We have also reported that PL preferentially targets PKCε in PCa DU-145 cells both *in vitro* and *in vivo* (Aziz et al., 2008). These finding prompted us to determine the effect of PL on the expression of PKCε and Stat3 in PC-3M luciferase cells derived orthotopic xenograft tumors.

PL treatment elicited a significant decrease in the expression of PKCε in excised orthotopic tumor tissues compared to control mice (Figure 5Ai–ii). In the same experiment, we also observed a significant decrease in the phosphorylation of both Tyr705 and Ser727 residues of Stat3 in excised orthotopic tumors of PL-treated group mice compared to control

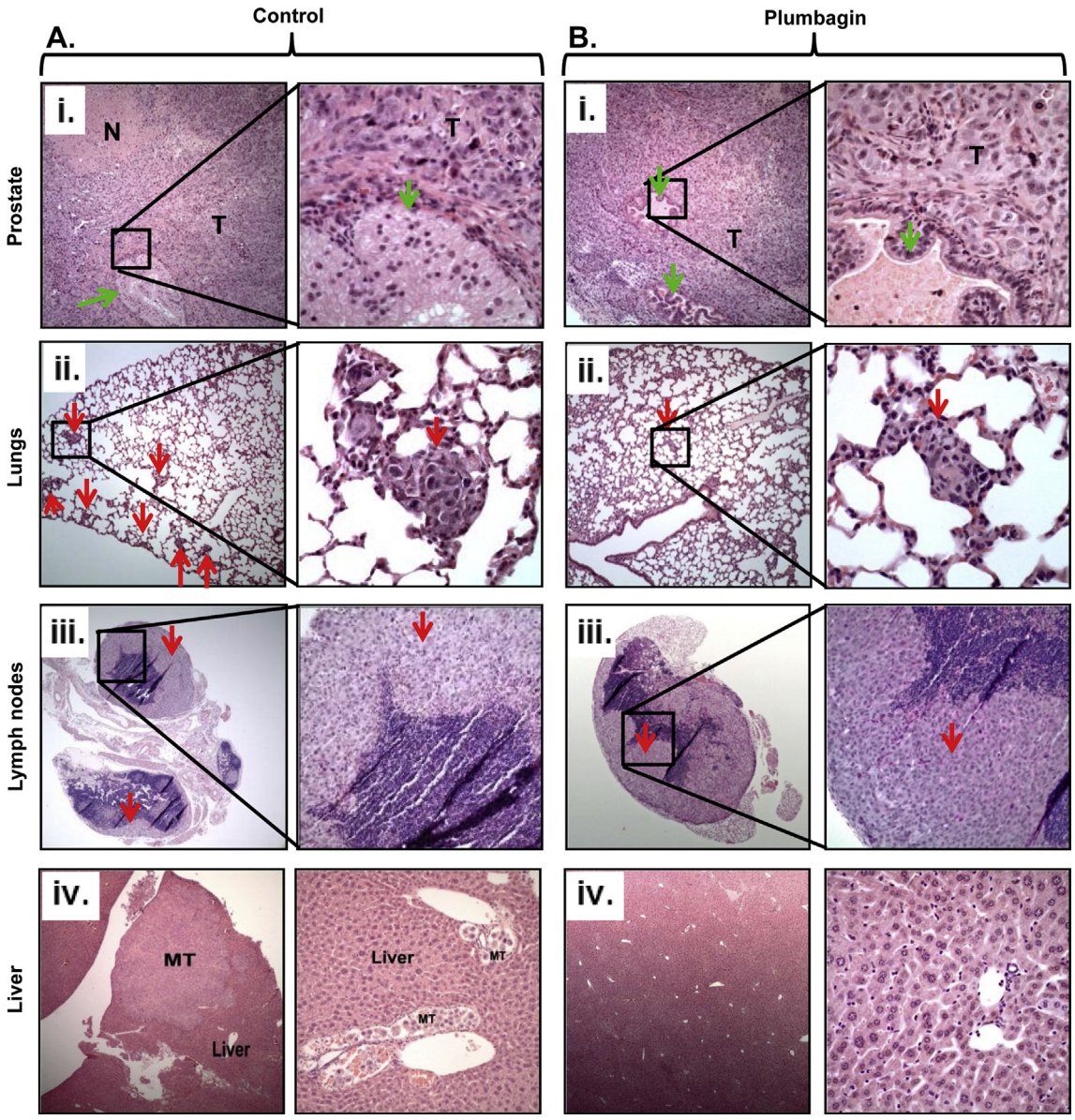

Figure 3 – Histopathology of excised prostate tumors, lungs, lymph nodes and liver of control and PL-treated mice. Ai and Bi: Representative photographs of H&E staining of excised prostates from vehicle treated (Ai) and PL-treated (Bi) mice at 8 week. T represents xenograft tumors arising from prostate, while green arrows denote to residual mouse prostate glands. Representative H&E staining pictures illustrating distant PCa metastasis into lungs (Aii) and lymph nodes (Aiii) of control mice. Multiple metastatic tumor foci were observed in these tissues as indicated by red arrows. PL-treated mice showed fewer tumor foci as shown in representative pictures of lungs (Bii), and lymph nodes (Biii), of PL-treated mice. Representative H&E staining pictures of control (Aiv) and PL-treated (Biv) animal liver. Control mice showed metastatic tumors in the liver as denoted by MT (Aiv).

mice (Figure 5Ai–ii). However, no significant effect was observed in the protein levels of total Stat3 (Figure 5Ai–ii).

Survivin and Bcl_{xL} are the downstream target genes of Stat3, which are involved in cell proliferation and inhibition of apoptosis respectively (Grandis et al., 2000; Gritsko et al., 2006). As shown in Figure 5Bi–ii, PL-treatment resulted in a significant inhibition of survivin and Bcl_{xL} expression in orthotopic xenograft tumor tissues compared to control mice.

3.3. *PL-treatment inhibits the expression of MMP2, MMP9, uPA, and induces iNOS expression in orthotopic xenograft tumors*

Activation of matrix metalloproteinase (MMPs), urokinase plasminogen activator (uPA), and angiogenic factors (VEGF and CD31) are shown to promote PCa metastasis into distant organs (Aalinkeel et al., 2011; Shariat et al., 2007; Boxler

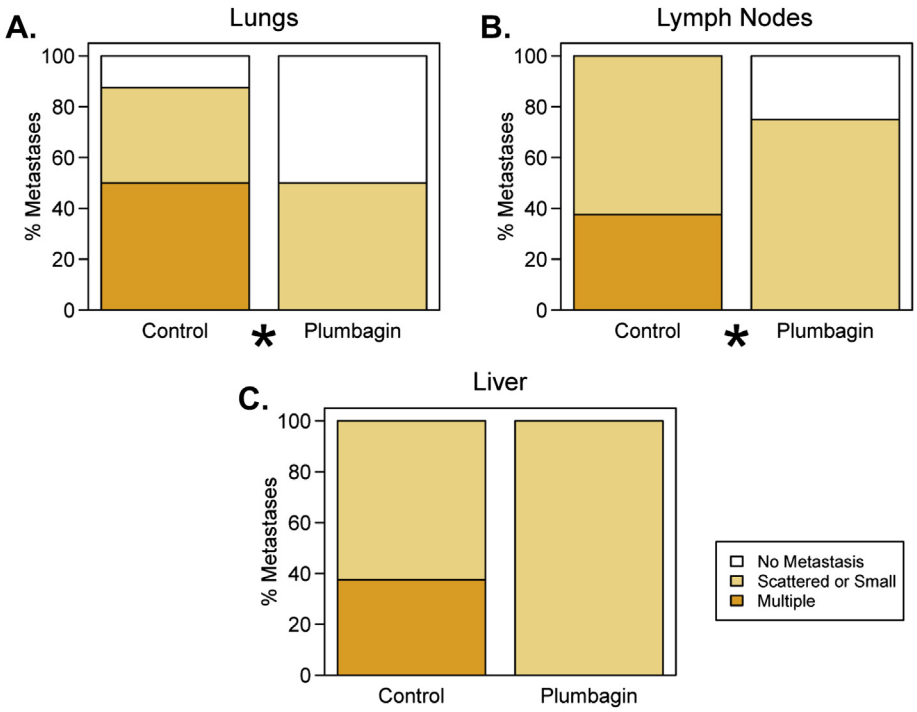

Figure 4 – Effect of PL-treatment on PCa metastasis into lungs, lymph nodes and liver. Histopathological evaluation of distant metastasis into lungs (A), lymph nodes (B) and liver (C). 100% stacked column graphs show the percent of single scattered, small metastatic cancer cells and multiple metastastic foci into the lungs (A), lymph nodes (B), and liver (C) of indicated groups.

et al., 2010). A possibility was explored whether PL-treatment inhibits the expression of MMP2, MMP9, VEGF and CD31 in excised orthotopic tumor tissues. Western blot analysis results indicated a significant decrease in MMP2, MMP9 expression in prostate tissues of PL-treated mice. (Figure 5Bi–ii). Similarly, PL-treatment resulted in decreased expression of VEGF (Figure 6Ai–ii) and CD31 (Figure 6Bi–ii). We further confirmed the expression of CD31 expression by Immunohistochemistry. Results also demonstrated a decrease expression of CD31 protein in excised prostate tissues of PL-treated mice (Figure 6Ci–ii). We further examined the effect of PL on other metastatic markers (E-Cadherin, uPA, and iNOS) in excised prostate tissues. Western blot analysis results showed a decrease expression of uPA in PL-treated excised prostate tissues (Figure 6Ei–ii). However, no change was observed in the expression of E-Cadherin compared to control (Figure 6D). Interestingly, we observed an increased expression of iNOS in all of the excised prostate tissues of PL-treated mice compared to control (Figure 6Ei–ii).

3.4. *PL-treatment inhibits expression of proliferative markers (Ki-67 and PCNA) in orthotopic xenograft tumors*

Overexpression of PCNA and Ki-67 are considered as prognostic biomarkers for various types of cancers including PCa (Liu et al., 2011; Zhao et al., 2011). We have shown that deletion of PKCε in TRAMP mice inhibits the expression of PCNA in prostate tissues (Hafeez et al., 2011). We analyzed the effect of PL-treatment on the expression of PCNA and Ki-67 in excised orthotopic tumors of both the group mice. Immunohistochemical analysis results showed inhibition of both PCNA (Figure 6Fi–ii) and Ki67 (Figure 6Gi–ii) expression in excised tumor tissues of PL-treated mice compared to control.

4. Discussion

Tumor progression toward metastasis is a multistage process in which malignant cells migrate from primary organs and colonize at distant organs (Nguyen et al., 2009). This metastasis process occurs through various mechanisms, including direct invasion of tumor cells into local or distant tissues by the lymphatic system or neovascularization (Steeg, 2006). Despite improvements in diagnosis, surgical techniques, and chemotherapies, most deaths of PCa patients occur due to disease progression and metastasis. Therefore, there is an urgent need to identify novel agents that could prevent the progression and metastasis of PCa. PL is a unique plant-derived naphthoquinone, isolated from the root of black walnut (Sandur et al., 2006), which has been shown for its potential health benefits including anti-tumor activity against various types of cancers (Padhye et al., 2012). We previously have shown that PL-administration delays ectopic growth of hormone-refractory PCa cells as well as reduces both tumor weight and volume by 90% (Aziz et al., 2008). Recently, we have reported chemopreventive effects of PL against PCa in TRAMP mice (Hafeez et al., 2012b). Here, we tested the hypothesis that PL has anti-metastasis property against human PCa.

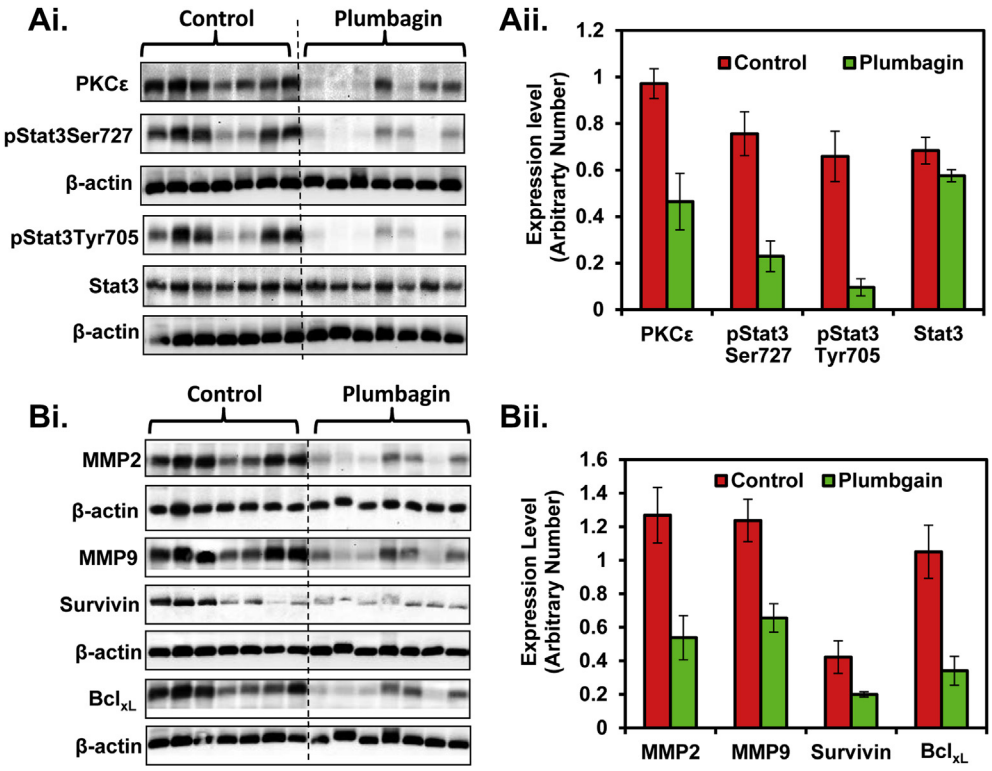

Figure 5 – Effect of PL-treatment on the expression of PKCε, Stat3, MMP2, MMP9, survivin and Bcl_{xL}. The expression level of the indicated protein was determined by Western blot analysis at eight week from the excised orthotopic xenograft tumor tissues of control and PL-treated mice. Each lane in the blot represents an individual mouse prostate tumor sample. Equal loading of protein was determined by stripping and re-probing the blots with actin antibody. Ai: Protein levels of PKCε, pStat3Ser727, pStat3Tyr705, and total Stat3. Bi: Protein levels of MMP2, MMP9, survivin and Bcl_{xL}Aii–Bii: Quantification of Western blots of Ai and Bi respectively. Blots were quantitated by densitometric analysis using TotalLab Nonlinear Dynamic Image analysis software.

In this study, we demonstrate anti-tumor growth and anti-metastatic properties of PL against human PCa. We have used human PCa PC3-M-luciferase cells to generate an orthotopic xenograft mouse model, which is an ideal model to study PCa progression and metastasis (Jenkins et al., 2003). The unique feature of this model is that a single metastatic luciferase labeled cell can be detected in live mice. Our experiments outcome from bioluminescence imaging of live mice clearly showed a significant ($p = 0.0008$) delay in growth of orthotopic tumors (Figure 1A–B). We also observed a significant ($p = 0.006$) decrease of orthotopic xenograft tumor weights in PL-treated mice (Figure 1D). These findings clearly demonstrate that PL treatment inhibits the progression of PC-3M-luciferase cells derived orthotopic xenograft tumors. In human, Lymph nodes, bones, lungs, and liver are the most frequent sites of PCa metastasis (Bubendorf et al., 2000). A recent study has suggested that liver metastasis predicts poor prognosis of metastasis castration resistant prostate cancer patients (Kelly et al., 2012). Interestingly, our data showed a significant ($p = 0.037$) inhibition of PC-3M-luciferase cells metastasis into the liver as determined by bioluminescence imaging. Histopathology analysis also showed a trend toward significance ($p = 0.075$) compared with control (Figure 2B). Metastasis trend of PCa cells toward lungs and lymph nodes was not significant (Figure 2B–C). This insignificant trend of PCa metastasis into lungs and lymph nodes was because of wide variance in between the different mice within each group. Although, we observed a big differences in the mean bioluminescence value of excised lungs and lymph nodes. Therefore, we did not attain statistical significant values of lungs and lymph nodes. Possibly, with the larger sample size could show us statistical significance, but at this point our data seems to be clinically significant. These findings are also in accord to the previously published reports, which have shown anti-metastatic potential of PL against breast cancer (Li et al., 2012; Sung et al., 2012). Although bones are the prime site of human PCa metastasis (Nguyen et al., 2009) but no previous published study has reported any bone metastasis in orthotopic xenograft mouse models of PCa. Our data also correspond to the previous published studies, as we also did not observe any bone metastasis in any of the mouse of both the groups (Figure 2Avii–viii). However, PCa bone metastasis could be investigated in another mouse model either implanting PCa cells directly into the bones or left ventricle of the heart (Rosol et al., 2003; Lee et al., 2012). Overall our data provide evidence of growth inhibitory and anti-metastatic nature of PL against human PCa.

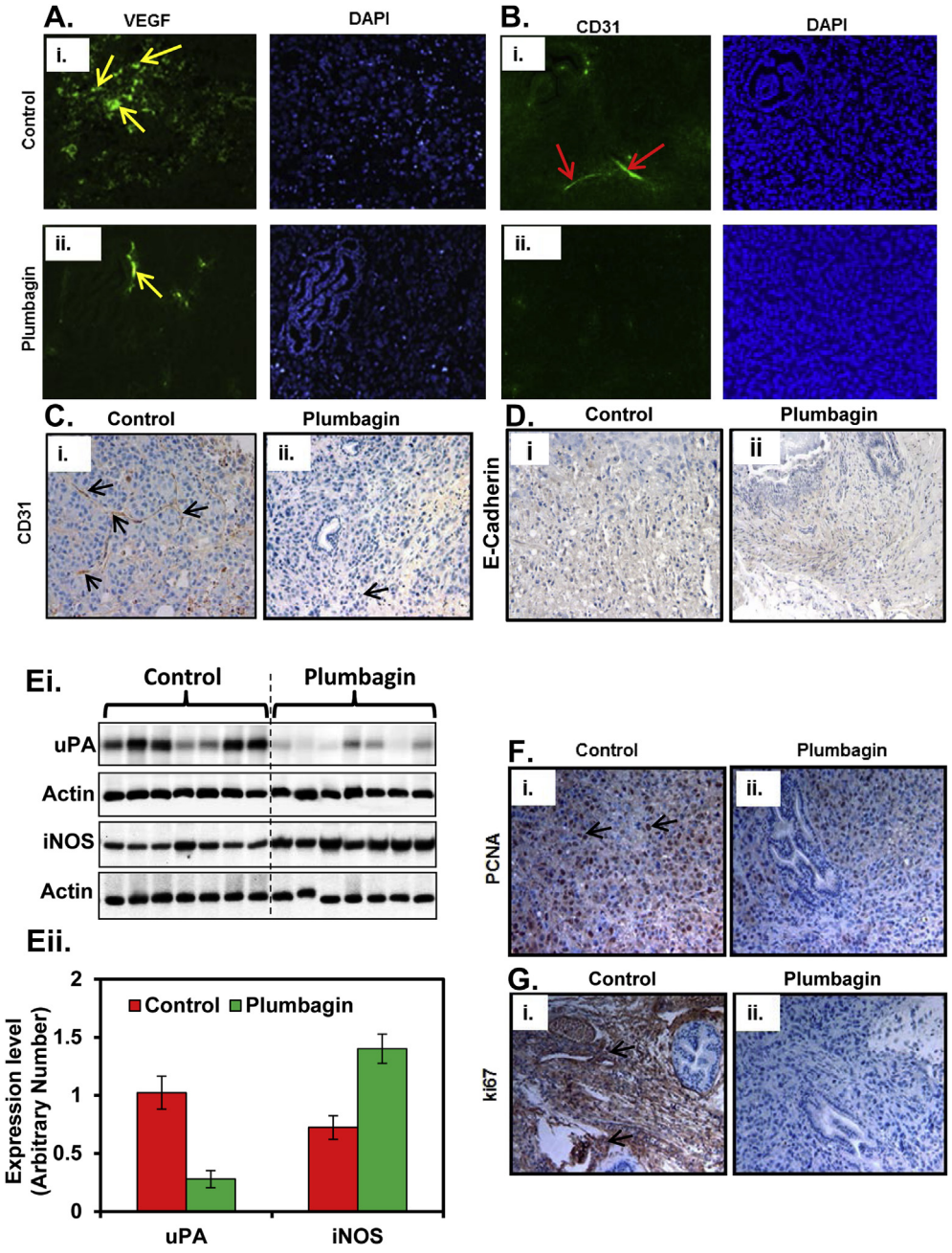

Figure 6 – Effect of PL-treatment on the expression of VEGF, CD31, uPA, iNOS and cell proliferation markers (Ki-67 and PCNA). A. Representative immunofluorescent images of VEGF expression in control (Ai) and PL-treated (Aii) mice excised xenograft tumor tissues. Yellow arrows indicate expression of VEGF. B. Representative immunofluorescent images of CD31 expression in control (Bi) and PL-treated (Bii) excised xenograft PCa tumor tissues. Red arrows indicate expression of CD31. C. Representative images of immunohistochemistry analysis of CD31 expression in control (Ci) and PL-treated (Cii) mice excised xenograft tumor tissues. Black arrows indicate expression of CD31 expression. D. Representative images of immunohistochemistry of E-Cadherin expression in control (Di) and PL-treated (Dii) mice excised xenograft PCa tumor tissues. E. uPA and iNOS expression in excised xenograft tumor tissues of individual mouse samples of indicated groups as determined by Western blot analysis (Ei). Equal loading of protein was determined by stripping and re-probing the blot with actin antibody (Ei). Quantification of Western blots by densitometric analysis using TotalLab Nonlinear Dynamic Image analysis software (Eii). F–G. Representative images of immunohistochemistry of PCNA (Fi–ii) and Ki-67 (Gi–ii) expression in excised xenograft tumor tissues of control and PL-treated mice.

The mechanism by which PL inhibits the development of PCa involves multiple targets including PKCε (Aziz et al., 2008). Evidence suggests that PKCε is an oncogene and plays an important role in the induction and progression of various types of cancers (Aziz et al., 2007b; Martínez-Gimeno et al., 1995; Pan et al., 2005) including PCa (Aziz et al., 2007a; Hafeez et al., 2011; Koren et al., 2004). Overexpression of PKCε is sufficient to promote conversion of androgen-dependent (AD) LNCaP cells to an androgen-independent (AI) variant, which rapidly initiates tumor growth *in vivo* in both

intact and castrated athymic nude mice (Wu et al., 2002). We have shown previously that PKCε expression correlates with the aggressiveness of human PCa (Aziz et al., 2007a) and genetic loss of PKCε in TRAMP mice prevents development and metastasis of PCa (Hafeez et al., 2011). A recent study suggests that overexpression of PKCε in mouse prostate epithelium develops prostatic intraepithelial neoplasia (PIN) at 16–18 weeks (Benavides et al., 2011). PKCε has also been linked to the regulation of various signaling pathways in PCa. Proteomic analysis of human PCa CWR22 cells xenografts show that the association of PKCε with Bax may neutralize apoptotic signals propagated through the mitochondrial death-signaling pathway (McJilton et al., 2003). We have shown that PKCε associated with Stat3 and this association increased with the PCa development and progression in human and TRAMP mouse model (Aziz et al., 2007a). Moreover, PKCε associates with Stat3 in other human cancer cell lines and targeted deletion of PKCε by using specific siRNA inhibits Stat3 phosphorylation at Ser727 in these cancer cell lines (Aziz et al., 2010). In TRAMP mice, we have shown that genetic loss of PKCε inhibits both Ser727 and Tyr705 Stat3 phosphorylation (Hafeez et al., 2011). These results prompted us to explore the effect of PL-treatment on Stat3 activation in PC-3M-lucifearse cells derived prostate tumor tissues. We observed that PL-treatment inhibits PKCε expression and Stat3 activation in orthotopic xenograft tumors in nude mice. Maximum activation of Stat3 requires phosphorylation of both the residues (Ser727 and Tyr705). Our data illustrated significant inhibitory effects of PL on pStat3Ser727 and pStat3Tyr705 in prostate tumor tissues (Figure 5Ai–ii). Our data also illustrated decrease expression of Stat3 downstream target genes (Bcl_{xL} and survivin) (Figure 5Bi–ii) in excised prostate tissues of PL-treated mice suggesting that PL targets Stat3 signaling in orthotopic xenograft tumors.

Prostate tumors progression from a localized disease occurs through a cascade of biological processes, including alteration in the cell proliferation, cell–cell adhesion, and the invasive potential of malignant cells. It is well documented that activation of Matrix metalloproteinases (MMPs) and increase uPA expression induces cancer cell migration and invasion in various types of human cancers including PCa (Boxler et al., 2010; Zhang et al., 2011). Our data showed inhibition of MMP2, MMP9 (Figure 5Bi–ii) and uPA (Figure 6Ei–ii) expression in orthotopic xenograft tumors of PL-treatment mice which could be one of the molecular mechanisms of PCa cells metastasis inhibition in orthotopic xenograft mouse model. A previous study has shown that intra-tumoral delivery of iNOS construct inhibits the growth of ectopic PC-3 cells xenograft tumors in athymic nude mice, which is associated with the production of NO in tumor cells (Coulter et al., 2010). Interestingly, our data showed increased expression of iNOS in excised prostate tissues of PL-treated mice. It may be possible that PL treatment induced NO production inside the tumor cells created cytotoxic environment to the tumor cells, which could be another possible molecular mechanism for tumor growth and metastasis inhibition in PC-3M-luciferase cells orthotopic xenograft mice. Our data also suggested a significant inhibition of proliferation marker PCNA and Ki-67 in orthotopic xenograft tumors. These findings are consistent with our previously published reports (Aziz et al., 2008; Hafeez et al., 2012b; Sand et al., 2012) and further suggest the strong anti-proliferative effects of PL against PCa.

In summary, we have used a clinically relevant orthotopic prostate tumor model to evaluate the effects of PL on tumor growth and metastasis of highly aggressive human PCa PC-3M-luciferase cells. We observed that PL significantly inhibited the growth and metastasis of PC-3M-luciferase cells in this pre-clinical mouse model. We conclude that PL may be a potential anti-metastatic agent for the treatment of human metastatic PCa.

Conflicts of interest

None.

Acknowledgment

This study was supported by NIH CA138761 grant to Ajit. K. Verma and UWCC Cancer Center Support grant 2P30CA014520-34 for small animal imaging and shared Biostatistics facilities.

Appendix A. Supplementary data

Supplementary data related to this article can be found at http://dx.doi.org/10.1016/j.molonc.2012.12.001.

REFERENCES

Aalinkeel, R., Nair, B.B., Reynolds, J.L., Sykes, D.E., Mahajan, S.D., Chadha, K.C., Schwartz, S.A., 2011. Overexpression of MMP-9 contributes to invasiveness of prostate cancer cell line LNCaP. Immunol. Invest. 40 (5), 447–464.

Albertsen, P., 2008. Predicting survival for men with clinically localized prostate cancer: what do we need in contemporary practice? Cancer 112, 1–3.

Aziz, M.H., Manoharan, H.T., Church, D.R., Dreckschmidt, N.E., Zhong, W., Oberley, T.D., Wilding, G., Verma, A.K., 2007a. Protein kinase C epsilon interacts with signal transducers and activators of transcription 3 (Stat3), phosphorylates Stat3Ser727, and regulates its constitutive activation in prostate cancer. Cancer Res. 67 (18), 8828–8838.

Aziz, M.H., Manoharan, H.T., Verma, A.K., 2007b. Protein kinase C epsilon, which sensitizes skin to sun's UV radiation-induced cutaneous damage and development of squamous cell carcinomas, associates with Stat3. Cancer Res. 67 (3), 1385–1394.

Aziz, M.H., Dreckschmidt, N.E., Verma, A.K., 2008. Plumbagin, a medicinal plant-derived naphthoquinone, is a novel inhibitor of the growth and invasion of hormone-refractory prostate cancer. Cancer Res. 68, 9024–9032.

Aziz, M.H., Hafeez, B.B., Sand, J.M., Pierce, D.B., Aziz, S.W., Dreckschmidt, N.E., Verma, A.K., 2010. Protein kinase C epsilon mediates Stat3Ser727 phosphorylation, Stat3-regulated gene expression, and cell invasion in various human cancer cell lines through integration with MAPK cascade (RAF-1, MEK1/2, and ERK1/2). Oncogene 29 (21), 3100–3109.

Benavides, F., Blando, J., Perez, C.J., Garg, R., Conti, C.J., DiGiovanni, J., Kazanietz, M.G., 2011. Transgenic overexpression of PKCε in the mouse prostate induces preneoplastic lesions. Cell Cycle 10 (2), 268–277.

Boxler, S., Djonov, V., Kessler, T.M., Hlushchuk, R., Bachmann, L.M., Held, U., Markwalder, R., Thalmann, G.N., 2010. Matrix metalloproteinases and angiogenic factors: predictors of survival after radical prostatectomy for clinically organ-confined prostate cancer? Am. J. Pathol. 177 (5), 2216–2224.

Bubendorf, L., Schöpfer, A., Wagner, U., Sauter, G., Moch, H., Willi, N., Gasser, T.C., Mihatsch, M.J., 2000. Metastatic patterns of prostate cancer: an autopsy study of 1,589 patients. Hum. Pathol. 31 (5), 578–583.

Coulter, J.A., Page, N.L., Worthington, J., Robson, T., Hirst, D.G., McCarthy, H.O., 2010. Transcriptional regulation of inducible nitric oxide synthase gene therapy: targeting early stage and advanced prostate cancer. J. Gene Med. 12 (9), 755–765.

Courboulin, A., Barrier, M., Perreault, T., Bonnet, P., Tremblay, V.L., Paulin, R., Tremblay, E., Lambert, C., Jacob, M.H., Bonnet, S.N., Provencher, S., Bonnet, S., 2012. Plumbagin reverses proliferation and resistance to apoptosis in experimental PAH. Eur. Respir. J. 40 (3), 618–629.

Gomathinayagam, R., Sowmyalakshmi, S., Mardhatillah, F., Kumar, R., Akbarsha, M.A., Damodaran, C., 2008. Anticancer mechanism of plumbagin, a natural compound, on non-small cell lung cancer cells. Anticancer Res. 28 (2A), 785–792.

Grandis, J.R., Drenning, S.D., Zeng, Q., Watkins, S.C., Melhem, M.F., Endo, S., Johnson, D.E., Huang, L., He, Y., Kim, J.D., 2000. Constitutive activation of Stat3 signaling abrogates apoptosis in squamous cell carcinogenesis in vivo. Proc. Natl. Acad. Sci. U.S.A 97 (8), 4227–4232.

Gritsko, T., Williams, A., Turkson, J., Kaneko, S., Bowman, T., Huang, M., Nam, S., Eweis, I., Diaz, N., Sullivan, D., Yoder, S., Enkemann, S., Eschrich, S., Lee, J.H., Beam, C.A., Cheng, J., Minton, S., Muro-Cacho, C.A., Jove, R., 2006. Persistent activation of stat3 signaling induces survivin gene expression and confers resistance to apoptosis in human breast cancer cells. Clin. Cancer Res. 12 (1), 11–19.

Hafeez, B.B., Zhong, W., Weichert, J., Dreckschmidt, N.E., Jamal, M.S., Verma, A.K., 2011. Genetic ablation of PKC epsilon inhibits prostate cancer development and metastasis in transgenic mouse model of prostate adenocarcinoma. Cancer Res. 71 (6), 2318–2327.

Hafeez, B.B., Jamal, M.S., Fischer, J.W., Mustafa, A., Verma, A.K., 2012a. Plumbagin, a plant derived natural agent inhibits the growth of pancreatic cancer cells in in vitro and in vivo via targeting EGFR, Stat3 and NF-κB signaling pathways. Int. J. Cancer 131 (9), 2175–2186.

Hafeez, B.B., Zhong, W., Mustafa, A., Fischer, J.W., Witkowsky, O., Verma, A.K., 2012b. Plumbagin inhibits prostate cancer development in TRAMP mice via targeting PKC{varepsilon}, Stat3 and neuroendocrine markers. Carcinogenesis 33 (12), 2586–2592.

Hsu, Y.L., Cho, C.Y., Kuo, P.L., Huang, Y.T., Lin, C.C., 2006. Plumbagin (5-hydroxy-2-methyl-1,4-naphthoquinone) induces apoptosis and cell cycle arrest in A549 cells through p53 accumulation via c-Jun NH2-terminal kinase-mediated phosphorylation at serine 15 in vitro and in vivo. J. Pharmacol. Exp. Ther. 318 (2), 484–494.

Jenkins, D.E., Yu, S.F., Hornig, Y.S., Purchio, T., Contag, P.R., 2003. In vivo monitoring of tumor relapse and metastasis using bioluminescent PC-3M-luc-C6 cells in murine models of human prostate cancer. Clin. Exp. Metastasis 20 (8), 745–756.

Kelly, W.K., Halabi, S., Carducci, M.A., George, D.J., Mahoney, J.F., Stadler, W.M., Morris, M.J., Kantoff, P.W., Monk, J.P., Small, E.J., 2012. Liver metastasis (LM) to predict for short overall survival (OS) in metastatic castration resistant prostate cancer (mCRPC) patients (pts). J. Clin. Oncol. 30 (Supp; abstract 4655).

Koren, R., Ben Meir, D., Langzam, L., Dekel, Y., Konichezky, M., Baniel, J., Livne, P.M., Gal, R., Sampson, S.R., 2004. Expression of protein kinase C isoenzymes in benign hyperplasia and carcinoma of prostate. Oncol. Rep. 11 (2), 321–326.

Lai, L., Liu, J., Zhai, D., Lin, Q., He, L., Dong, Y., Zhang, J., Lu, B., Chen, Y., Yi, Z., Liu, M., 2012. Plumbagin inhibits tumour angiogenesis and tumour growth through the Ras signalling pathway following activation of the VEGF receptor-2. Br. J. Pharmacol. 165 (4b), 1084–1096. http://dx.doi.org/10.1111/j.1476-5381.2011.01532.x.9 [Epub ahead of print].

Lee, H.J., Yu, H.K., Papadopoulos, J.N., Kim, S.W., He, J., Park, Y.K., Yoon, Y., Kim, J.S., Kim, S.J., 2012. Targeted antivascular therapy with the apolipoprotein(a) kringle V, rhLK8, inhibits the growth and metastasis of human prostate cancer in an orthotopic nude mouse model. Neoplasia 14 (4), 335–343.

Li, Z., Xiao, J., Wu, X., Li, W., Yang, Z., Xie, J., Xu, L., Cai, X., Lin, Z., Guo, W., Luo, J., Liu, M., 2012. Plumbagin inhibits breast tumor bone metastasis and osteolysis by modulating the tumor-bone microenvironment. Curr. Mol. Med. 8, 967–981.

Liu, C., Liu, J., Wang, X., Mao, W., Jiang, L., Ni, H., Mo, M., Wang, W., 2011. Prognostic impact of nm23-H1 and PCNA expression in pathologic stage I non-small cell lung cancer. J. Surg. Oncol. 104 (2), 181–186.

Martínez-Gimeno, C., Díaz-Meco, M.T., Domínguez, I., Moscat, J., 1995. Alterations in levels of different protein kinase C isotypes and their influence on behavior of squamous cell carcinoma of the oral cavity: epsilon PKC, a novel prognostic factor for relapse and survival. Head Neck 17 (6), 516–525.

McJilton, M.A., Van Sikes, C., Wescott, G.G., 2003. Protein kinase C epsilon interacts with Bax and promotes survival of human prostate cancer cells. Oncogene 22, 7958–7968.

Nguyen, D.X., Bos, P.D., Massagué, J., 2009. Metastasis: from dissemination to organ-specific colonization. Nat. Rev. Cancer 9 (4), 274–284.

Padhye, S., Dandawate, P., Yusufi, M., Ahmad, A., Sarkar, F.H., 2012. Perspectives on medicinal properties of plumbagin and its analogs. Med. Res. Rev. 32 (6), 1131–1158.

Pan, Q., Bao, L.W., Kleer, C.G., Sabel, M.S., Griffith, K.A., Teknos, T.N., Merajver, S.D., 2005. Protein kinase C epsilon is a predictive biomarker of aggressive breast cancer and a validated target for RNA interference anticancer therapy. Cancer Res. 65 (18), 8366–8371.

Powolny, A.A., Singh, S.V., 2008. Plumbagin-induced apoptosis in human prostate cancer cells is associated with modulation of cellular redox status and generation of reactive oxygen species. Pharm. Res. 25 (9), 2171–2180.

R. Core Development Team, 2011. R: a Language and Environment for Statistical Computing. R Foundation for Statistical Computing, Vienna, Austria, ISBN 3-900051-07-0. URL. http://www.R-project.org.

Ravindra, K.C., Selvi, B.R., Arif, M., Reddy, B.A., Thanuja, G.R., Agrawal, S., Pradhan, S.K., Nagashayana, N., Dasgupta, D., Kundu, T.K., 2009. Inhibition of lysine acetyltransferase KAT3B/p300 activity by a naturally occurring hydroxynaphthoquinone, plumbagin. J. Biol. Chem. 284 (36), 24453–24464.

Rosol, T.J., Tannehill-Gregg, S.H., LeRoy, B.E., Mandl, S., Contag, C.H., 2003. Animal models of bone metastasis. Cancer 97 (Suppl. 3), 748–757. Review.

Sand, J.M., Hafeez, B.B., Jamal, M.S., Witkowsky, O., Siebers, E.M., Fischer, J., Verma, A.K., 2012. Plumbagin (5-hydroxy-2-methyl-1,4-naphthoquinone), isolated from Plumbago zeylanica, inhibits ultraviolet radiation-induced development of squamous cell carcinomas. Carcinogenesis 33 (1), 184–190.

Sandur, S.K., Ichikawa, H., Sethi, G., Ahn, K.S., Aggarwal, B.B., 2006. Plumbagin (5-hydroxy-methyl-1,4-naphthoquinone) suppresses NF-kappaB activation and NF-kappaB-regulated gene products through modulation of p65 and lkappaBalpha

kinase activation, leading to potentiation of apoptosis induced by cytokine and chemotherapeutic agents. J. Biol. Chem. 281, 17023–17033.

Shariat, S.F., Roehrborn, C.G., McConnell, J.D., Park, S., Alam, N., Wheeler, T.M., Slawin, K.M., 2007. Association of the circulating levels of the urokinase system of plasminogen activation with the presence of prostate cancer and invasion, progression, and metastasis. J. Clin. Oncol. 25 (4), 349–355.

Siegel, R., Naishadham, D., Jemal, A., 2012. Cancer statistics, 2012. CA Cancer J. Clin. 62 (1), 10–29.

Sinha, S., Pal, K., Elkhanany, A., Dutta, S., Cao, Y., Mondal, G., Iyer, S., Somasundaram, V., Couch, F.J., Shridhar, V., Bhattacharya, R., Mukhopadhyay, D., Srinivas, P., 2012 Jul 17. Plumbagin inhibits tumorigenesis and angiogenesis of ovarian cancer cells in vivo. Int. J. Cancer. http://dx.doi.org/10.1002/ijc.27724 [Epub ahead of print].

So, A., Gleave, M., Hurtado-Col, A., Nelson, C., 2005. Mechanisms of the development of androgen independence in prostate cancer. World J. Urol. 23, 1–9.

Son, T.G., Camandola, S., Arumugam, T.V., Cutler, R.G., Telljohann, R.S., Mughal, M.R., Moore, T.A., Luo, W., Yu, Q.S., Johnson, D.A., Johnson, J.A., Greig, N.H., Mattson, M.P., 2010. Plumbagin, a novel Nrf2/ARE activator, protects against cerebral ischemia. J. Neurochem. 112 (5), 1316–1326.

Steeg, P.S., 2006. Tumor metastasis: mechanistic insights and clinical challenges. Nat. Med. 12 (8), 895–904.

Sugie, S., Okamoto, K., Rahman, K.M., Tanaka, T., Kawai, K., Yamahara, J., Mori, H., 1998. Inhibitory effects of plumbagin and juglone on azoxymethane-induced intestinal carcinogenesis in rats. Cancer Lett. 127 (1–2), 177–183.

Sung, B., Oyajobi, B., Aggarwal, B.B., 2012. Plumbagin inhibits osteoclastogenesis and reduces human breast cancer-induced osteolytic bone metastasis in mice through suppression of RANKL signaling. Mol. Cancer Ther. 11 (2), 350–359.

Wang, C.C., Chiang, Y.M., Sung, S.C., Hsu, Y.L., Chang, J.K., Kuo, P.L., 2008. Plumbagin induces cell cycle arrest and apoptosis through reactive oxygen species/c-Jun N-terminal kinase pathways in human melanoma A375.S2 cells. Cancer Lett. 259, 82–98.

Wu, D., Foreman, T.L., Gregory, C.W., McJilton, M.A., Wescott, G.G., Ford, O.H., Alvey, R.F., Mohler, J.L., Terrian, D.M., 2002. Protein kinase C epsilon has the potential to advance the recurrence of human prostate cancer. Cancer Res. 62 (8), 2423–2429.

Zhang, J., Sud, S., Mizutani, K., Gyetko, M.R., Pienta, K.J., 2011. Activation of urokinase plasminogen activator and its receptor axis is essential for macrophage infiltration in a prostate cancer mouse model. Neoplasia 13 (1), 23–30.

Zhao, H., Lo, Y.H., Ma, L., Waltz, S.E., Gray, J.K., Hung, M.C., Wang, S.C., 2011. Targeting tyrosine phosphorylation of PCNA inhibits prostate cancer growth. Mol. Cancer Ther. 10 (1), 29–36.